Functional cysteine-less subunits of the transporter associated with antigen processing (TAP1 and TAP2) by de novo gene assembly

Susanne Heintke[a], Min Chen[a], Ulrike Ritz[b], Brigitte Lankat-Buttgereit[c], Joachim Koch[a], Rupert Abele[a], Barbara Seliger[b], Robert Tampé[a,*]

[a] *Institut für Biochemie, Biozentrum, Johann Wolfgang Goethe-Universität Frankfurt, Marie Curie Str. 9, D-60439 Frankfurt/M, Germany*
[b] *III. Med. Klinik and Poliklinik, Johannes Gutenberg-Universität Klinikum Mainz, Langenbeckstr. 1, D-55131 Mainz, Germany*
[c] *Institut für Physiologische Chemie, Philipps-Universität Marburg, Karl-von-Frisch-Str. 1, D-35043 Marburg, Germany*

Received 17 October 2002; accepted 21 November 2002

First published online 3 December 2002

Edited by Irmgard Sinnig

Abstract Within the adaptive immune system the transporter associated with antigen processing (TAP) plays a pivotal role in loading of peptides onto major histocompatibility (MHC) class I molecules. As a central tool to investigate the structure and function of the TAP complex, we created cysteine-less human TAP subunits by de novo gene synthesis, replacing all 19 cysteines in TAP1 and TAP2. After expression in TAP-deficient human fibroblasts, cysteine-less TAP1 and TAP2 are functional with respect to adenosine triphosphate (ATP)-dependent peptide transport and inhibition by ICP47 from herpes simplex virus. Cysteine-less TAP1 and TAP2 restore maturation and intracellular trafficking of MHC class I molecules to the cell surface.

Key words: Adenosine triphosphate-binding cassette transporter; Antigen processing; Cysteine-scanning mutagenesis; Membrane protein

1. Introduction

The translocation of proteasomal proteolytic peptides from the cytosol into the endoplasmic reticulum (ER) is a crucial step in antigen processing and presentation to cytotoxic T-lymphocytes (CTLs). This task is performed by the transporter associated with antigen processing (TAP). In the ER lumen, these peptides are loaded onto major histocompatibility (MHC) complex class I molecules and subsequently shuttled to the plasma membrane (for review see [1,2]). Efficient peptide loading of MHC class I molecules requires a macromolecular loading complex which includes TAP, tapasin, MHC class I molecules and several other assembling factors [3,4]. Peptide-loaded MHC complexes are released to the cell surface, where they are inspected by CTLs, which eventually lead to lysis/apoptosis of the malignant or infected cell [1].

TAP belongs to the family of ATP-binding cassette (ABC) transporters that translocate a broad spectrum of solutes across membranes in an ATP-dependent manner. The TAP complex located in the ER membrane is a heterodimer comprised of TAP1 and TAP2. Each subunit consists of a hydrophobic transmembrane domain (TMD) followed by a hydrophilic conserved cytosolic nucleotide-binding domain (NBD) (for review see [5,6]). Sequence alignments and hydrophobicity analyses predict 10 transmembrane helices for human TAP1 and nine for human TAP2 [5]. The N-terminus of TAP1 is most probably directed towards the cytosol, whereas the N-terminus of TAP2 faces the ER lumen [7].

Both TAP subunits are essential for peptide transport and no additional factors of the adaptive immune system are required [8,9]. Consequently, a lack of one TAP subunit leads to a non-functional transporter and inefficient peptide loading of MHC class I molecules and their retention in the ER [10–12]. The TAP complex preferentially recognizes peptides of 8–16 amino acids [13]. The transport mechanism by TAP can be divided into two basic steps: ATP-independent peptide binding and ATP-dependent peptide translocation across the ER membrane [5,13,14].

The interdependency between peptide binding, transport and release, its synchronization with ATP binding and hydrolysis have been recently investigated [15–18]. However, many questions concerning structure, dynamics and mechanism of the TAP complex remain open. Cysteine-less TAP mutants will be a powerful tool to address these topics [19]. Applying cysteine-scanning mutagenesis, the membrane topology and dynamic crosstalk between both NBDs and TMDs can be analyzed while preserving function and topology of the transporter investigated.

In this study, we report the de novo gene synthesis and functional expression of cysteine-less TAP1 and TAP2 subunits. In vitro transport assays demonstrate that cysteine-less and wild-type TAP1 and TAP2 are functionally equivalent with regard to ATP-dependent peptide translocation into the ER and inhibition by the herpes viral inhibitor ICP47. We were able to restore TAP-dependent peptide transport in vivo and to induce upregulation of MHC class I expression at the cell surface by transfection of cysteine-less TAP1 and TAP2 in TAP-deficient human skin fibroblasts.

2. Materials and methods

2.1. De novo synthesis of the cysteine-less TAP1 and TAP2

Partially overlapping oligonucleotides (60 bp in length and 15 bp overlap at both ends) were synthesized (Syngen-Biotech, Munich, Germany). Five double-stranded DNA fragments (400–450 bp) of

*Corresponding author. Fax: (49)-69-798 29495.
E-mail address: tampe@em.uni-frankfurt.de (R. Tampé).

Abbreviations: ECL, enhanced chemiluminescence; FACS, fluorescence-activated cell sorting; MHC, major histocompatibility complex; NBD, nucleotide-binding domain; TAP, transporter associated with antigen processing; TMD, transmembrane domain

0014-5793/02/$22.00
PII: S0014-5793(02)03746-8

each TAP subunit were generated by polymerase chain reactions. The DNA fragments were cloned into the vector pCR-Script (Stratagene) and sequenced. By using unique restriction sites, the fragments were assembled to the complete cDNA coding for cysteine-less TAP1 and TAP2. Finally, de novo genes were subcloned into the expression vector p46 (pCMVires Neo-derivative) and confirmed by sequencing. De novo *tap1* and *tap2* were constructed with a C-terminal His_{10}-tag and Strep®-tag, respectively. The plasmids were named as p46.TAP1dn and p46.TAP2dn. In addition, wild-type *tap1* and *tap2* were cloned into the expression vector p46.

2.2. Cell lines and culture

TAP1-deficient BRE cells (BRE.TAP1−/−) and TAP2-deficient STF cells (STF.TAP2−/−) were kindly provided by Henri de la Salle [12] and maintained in Dulbecco's modified Eagle's medium (DMEM) supplemented with 10% fetal calf serum (FCS), 2 mM L-glutamine, 100 μg/ml streptomycin and 100 U/ml penicillin.

2.3. Stable transfection of TAP-deficient cells

24 h after plating of 1×10^5 BRE.TAP1−/− and STF.TAP2−/− cells, the cells were transfected with 0.5 μg of linearized plasmid DNA (p46.TAP1dn or p46.TAP1wt and p46.TAP2dn or p46.TAP2wt) using the Effectene Transfection Kit (Qiagen). Cells were selected in DMEM (see Section 2.2) supplemented with 100 μg/ml hygromycin B and 500 μg/ml G418. The medium was exchanged every second day. After 5–6 weeks, G418-resistant positive cell clones were isolated and expanded for further analysis. Stable BRE transfectants were named as BRE.TAP1dn or BRE.TAP1wt, stable STF transfectants were indicated as STF.TAP2dn or STF.TAP2wt.

2.4. Membrane preparation and Western blot analysis

Approximately 1×10^7 cells were resuspended in 10 mM Tris buffer (pH 8.0) containing 1 mM dithiothreitol, 10 μg/ml aprotinin, 9.5 μg/μl leupeptin, 17 μg/μl pepstatin, 50 μg/ml phenylmethylsulfonyl fluoride and 10 μg/ml trypsin inhibitor and homogenized with a tight glass Dounce homogenizer (Braun, Melsungen, Germany). Cell debris was removed by centrifugation at $1000\times g$ for 10 min at 4°C. The supernatant was subsequently centrifuged at $200\,000\times g$ for 40 min at 4°C. Proteins of the membrane fraction were separated by sodium dodecyl sulfate–polyacrylamide gel electrophoresis (SDS–PAGE) (9%) and analyzed by immunoblotting. TAP1 was detected by enhanced chemiluminescence (ECL) using mAb148.3 [8] and a peroxidase-conjugated anti-mouse antibody (Sigma-Aldrich).

2.5. Peptide transport assay

The peptide RRYQNSTEL was labeled with ^{125}I by chloramine T as previously described [8]. 2.5×10^6 cells were semi-permeabilized with 0.05% (w/v) saponin in 50 μl transport buffer (20 mM HEPES, 130 mM KCl, 10 mM NaCl, 1 mM $CaCl_2$, 2 mM ethyleneglycol-bis-(β-aminoethylether)-*N*,*N*,*N*′,*N*′-tetraacetic acid (EGTA), 2 mM $MgCl_2$, pH 7.3) for 1 min at room temperature and subsequently diluted in 1 ml of transport buffer, centrifuged and washed with transport buffer. The peptide transport assay was started by adding 10 mM ATP and 0.8 μM of radiolabeled peptide in a final volume of 100 μl. After incubation at 37°C for 20 min, the cells were lysed in lysis buffer (50 mM Tris, 150 mM NaCl, 5 mM KCl, 1 mM $CaCl_2$, 2 mM $MnCl_2$, 1% IGEPAL, pH 7.5). The N-core glycosylated and therefore transported peptides were recovered with concanavalin A (ConA)-Sepharose beads (Sigma-Aldrich) overnight at 4°C [20]. After washing in lysis buffer, ConA-bound radiolabeled peptides were quantified by γ-counting.

2.6. Flow cytometry

MHC class I surface expression was monitored by fluorescence-activated cell sorting (FACS) analysis. 5×10^5 cells were harvested, washed twice with phosphate-buffered saline (PBS), and then incubated for 30 min on ice with the antibody HLA-ABC-FITC (Beckman/Coulter), which is specific for all MHC class I subtypes. For isotypic control, cells were incubated with the antibody IgG_{2a}-FITC (Beckman/Coulter). After washing with PBS, 5000 viable cells were analyzed by flow cytometry (Coulter Epics XL MCL using System II 3.0; Beckman/Coulter).

3. Results and discussion

3.1. Cloning of cysteine-less TAP subunits and generation of stable transfectants

To create cysteine-less human TAP, the *tap* genes were synthesized by partially overlapping oligonucleotides and PCR reactions as described in Section 2. By using unique restriction sites five PCR fragments were assembled to the complete de novo *tap1* (2298 bp, C-terminal His_{10}-tag) and de novo *tap2* sequence (2163 bp, C-terminal Strep®-tag). All cysteines, nine of TAP1 and 10 of TAP2, were replaced by de novo gene synthesis and assembly (Fig. 1). Cysteines were substituted

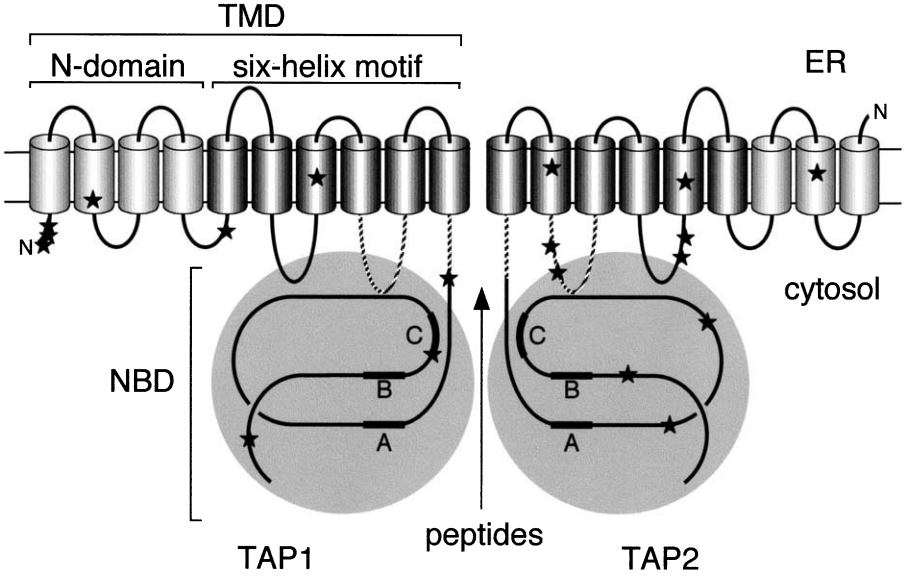

Fig. 1. Structural organization of the human TAP complex. The membrane helices are predicted from hydrophobicity analysis and sequence alignment with human MDR1 [5]. The N-terminal domain (N-domain) and the classical six-helix motif found in most ABC transporters of the TMD are illustrated in light and dark gray cylinders, respectively. The NBD consists of the highly conserved Walker A and B motifs (A, B) and the C-loop (C). Dashed lines illustrate the peptide-binding region as identified by photo-cross-linking experiments [23]. Asterisks indicate the location of the nine and 10 cysteines within TAP1 and TAP2, respectively.

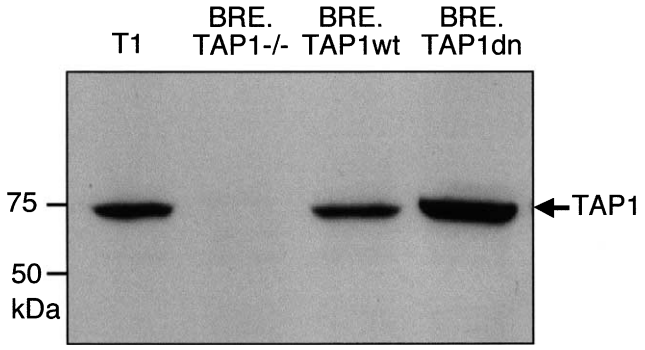

Fig. 2. Expression of cysteine-less TAP1. Proteins (30 μg/lane) obtained from membrane preparation of T1, BRE.TAP1−/−, BRE.TAP1wt and BRE.TAP1dn cells were separated by SDS–PAGE (9%), blotted onto a nitrocellulose membrane, probed with the anti-hTAP1 mAb148.3 [8] and visualized by means of ECL detection reagent.

by serines (C6S, C12S, C14S, C73S, C179S, C488S, C662S, C735S of TAP1; C70S, C213S, C353S, C363S, C571S, C641S of TAP2); however, cysteines located within predicted transmembrane helices were exchanged to alanines (C315A of TAP1; C197A, C209A of TAP2). Based on sequence alignments among TAP homologs from other species, two cysteines in TAP2 were replaced by histidine and valine (C394V and C540H). It should be stressed that none of the cysteines is conserved within TAP proteins from other species. Furthermore, based on the predicted membrane topology, no cysteine residue is located in the ER lumen, which could be involved in disulfide formation. By introducing unique restriction sites via silent mutations, de novo *tap1* and *tap2* were subdivided into gene cassettes of 150–250 bp each, which can easily be mutagenized and exchanged. In addition, the codon usage of the de novo *tap1* and *tap2* was optimized for expression in *Escherichia coli*, *Saccharomyces cerevisiae* and mammalian cells.

De novo (cysteine-less) and wild-type *tap1* or *tap2* were cloned into the expression vector p46 and transfected into human skin fibroblasts, BRE.TAP1−/− or STF.TAP2−/−, lacking TAP1 or TAP2 expression, respectively [12]. Genomic integration of the de novo *tap1* and *tap2* genes leading to G418-resistant BRE.TAP1dn or STF.TAP2dn cell lines was proven by genomic PCR (data not shown). For control experiments, wild-type TAP1 or TAP2 transfectants of both TAP-deficient cell lines were generated (BRE.TAP1wt or STF.TAP2wt).

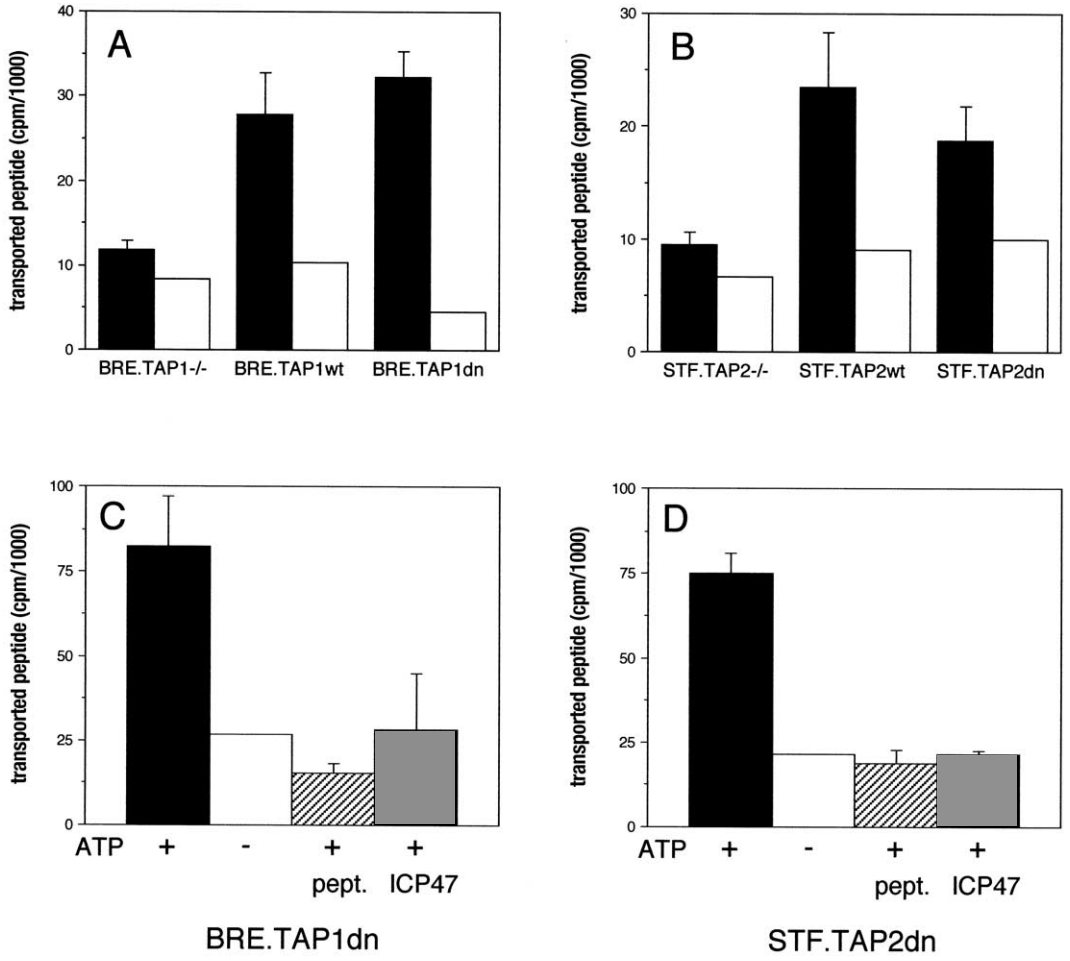

Fig. 3. ATP-dependent peptide transport by cysteine-less TAP1 and TAP2. The translocation assay was performed with 0.8 μM I^{125}-labeled peptide (RRYQNSTEL) for 20 min at 37°C in presence (dark bars) and absence of 10 mM MgATP (open bars) using 2.5×10^6 saponin semi-permeabilized BRE.TAP1−/−, BRE.TAP1wt, BRE.TAP1dn (A), as well as STF.TAP2−/−, STF.TAP2wt and STF.TAP2dn cells (B). The transported and glycosylated peptides (ConA-bound) were quantified by γ-counting. Similar in vitro transport assays were performed in the presence of a competitor peptide (160 μM of RRYQNSTEL, dashed bars) or the viral TAP inhibitor ICP47 (20 μM, gray bars) with BRE.TAP1dn (C) and STF.TAP2dn transfectants (D). Error bars indicate the deviation of two independent experiments.

Expression of cysteine-less and wild-type TAP1 was demonstrated by SDS–PAGE and Western blot analysis using the monoclonal antibody 148.3 directed against the C-terminus of human TAP1 [8]. In membrane preparations of all BRE transfectants and T1 cells (positive control), TAP1 was detected at the expected size of 71 kDa, whereas the parental BRE.TAP1−/− cell line showed no TAP1 expression (Fig. 2). De novo and wild-type TAP1 show the same apparent molecular mass.

Expression of cysteine-less and wild-type TAP2 was analyzed in STF cells using the monoclonal antibody 429.3 specific for human TAP2 [13]. However, TAP2 appears to be expressed at very low level in transfected STF.TAP2wt and STF.TAP2dn cells and could therefore not be detected. The immune detection of TAP2 could not be improved by using other monoclonal or polyclonal antibodies. Even though TAP2 expression is limiting for the formation of TAP1/TAP2 heterodimers, the amount of functional transporters is sufficient to be detected in assays addressing peptide transport and restoration of MHC class I surface expression (see below).

3.2. Function of cysteine-less TAP1 and TAP2

The intracellular transport of peptides into the ER lumen is a central step in antigen processing. To investigate whether the substitution of cysteines has an effect on TAP function, in vitro peptide transport assays were performed with saponin semi-permeabilized BRE and STF fibroblasts. ATP-dependent transport of the radiolabeled peptide (RRYQNSTEL) into the ER was analyzed in the presence and absence of ATP. After cell lysis, transported and N-core glycosylated peptides were quantified by γ-counting. As shown in Fig. 3A, ATP-dependent peptide transport was restored in cysteine-less and wild-type TAP1 transfectants (BRE.TAP1dn and BRE.TAP1wt), whereas no specific transport activity was observed in parental BRE.TAP1−/− fibroblasts. The transport efficiencies of the TAP complex comprising wild-type and de novo TAP1 were comparable, indicating that the replacement of all nine cysteines within the TAP1 had no effect on TAP transport function.

ATP-dependent peptide translocation was also observed for de novo and wild-type TAP2 transfectants, indicating that the exchange of 10 cysteines within TAP2 did not interfere with TAP transport function (Fig. 3B). We did not detect specific transport activity in case of the TAP2-deficient cell line (STF.TAP2−/−). Similar results were obtained for several clones of *tap1* or *tap2* transfectants.

Next, we analyzed whether the exchange of cysteines in human TAP1 or TAP2 affects the high-affinity interaction with ICP47 from herpes simplex virus, which specifically blocks peptide binding and translocation by human TAP [21,22]. As shown in Fig. 3C and D, ICP47 specifically blocks peptide translocation of cysteine-less TAP1 and TAP2. Similar inhibition was achieved by a 200-fold excess of unlabeled peptide. In summary, exchange of all 19 cysteines in both TAP subunits maintains TAP function as well as sensitivity towards the viral inhibitor ICP47.

3.3. Restoration of MHC class I surface expression by cysteine-less TAP1 and TAP2

After translocation of peptides into the ER lumen and subsequent loading onto MHC class I molecules, the peptide–MHC complexes are shuttled to the plasma membrane. Thus, the level of MHC class I surface expression serves as a readout for a functional antigen processing machinery. To analyze whether cysteine-less TAP subunits can restore maturation and intracellular trafficking of MHC I complexes, we determined the surface expression of MHC class I molecules by FACS analysis. The specific fluorescence intensity for

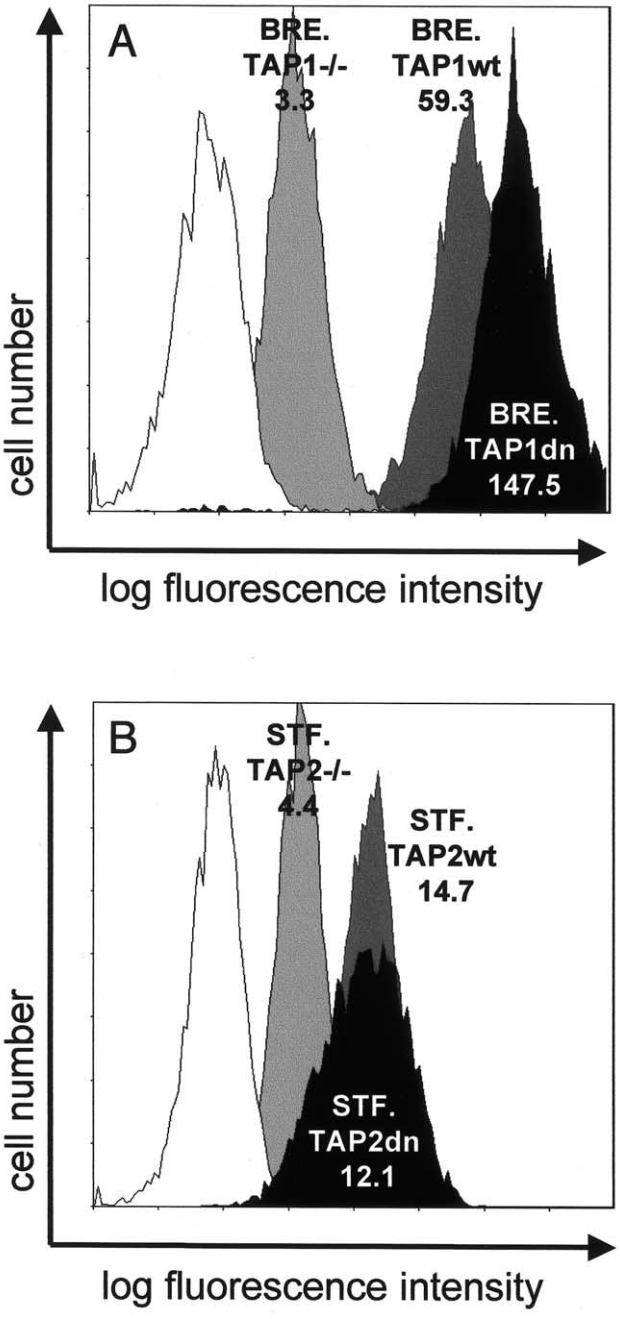

Fig. 4. Restoration of MHC class I surface expression by cysteine-less TAP1 and TAP2. To analyze antigen processing in BRE.TAP1−/−, BRE.TAP1wt, BRE.TAP1dn (A) as well as STF.TAP2−/−, STF.TAP2wt and STF.TAP2dn cell lines (B), the MHC class I expression on the cell surface was studied by FACS analysis using the anti-MHC class I antibody HLA-ABC-FITC. The antibody IgG_{2a}-FITC was used for isotopic control (white graph). One representative experiment out of at least two independent measurements for each cell line is shown.

transfected BRE.TAP1wt cells was determined to be 59.3, which is characteristic for a functional and efficient pathway of antigen presentation (Fig. 4A). Furthermore, MHC class I surface expression was shown for the cysteine-less TAP-transfected BRE cells with a higher fluorescence intensity of 147.5 when compared to the BRE.TAP1wt cell line. As expected the parental TAP1-deficient BRE cells showed largely suppressed MHC class I surface expression (log fluorescence intensity 3.3).

Similarly, the TAP2-transfected STF cell lines were analyzed by FACS. The specific fluorescence intensity for the STF.TAP2wt cell line was determined to be 14.7, whereas the cysteine-less TAP2 transfectants displayed a marginally lower specific fluorescence intensity of 12.1 (Fig. 4B). The parental TAP2-deficient STF cells showed strongly reduced MHC class I surface expression (log fluorescence intensity 4.4).

In summary, we show that the replacement of all cysteines within TAP1 and TAP2 has no effect on peptide transport, maturation and intracellular trafficking of MHC class I molecules to the cell surface. We therefore conclude that both cysteine-less TAP subunits preserve their functionality as key players in the pathway of antigen presentation. Cysteine-less TAP is an important tool and prerequisite for the investigation of structure, dynamics and transport mechanism of TAP as well as the overall organization of the macromolecular MHC loading complex.

Acknowledgements: We thank Eckhard Linker for excellent technical support. The work was supported by the Deutsche Forschungsgemeinschaft and the Fonds der Chemischen Industrie.

References

[1] Pamer, E. and Cresswell, P. (1998) Annu. Rev. Immunol. 16, 323–358.
[2] Lankat-Buttgereit, B. and Tampé, R. (2002) Physiol. Rev. 82, 187–204.
[3] Ortmann, B., Copeman, J., Lehner, P.J., Sadasivan, B., Herberg, J.A., Grandea, A.G., Riddell, S.R., Tampé, R., Spies, T. and Trowsdale, J. (1997) Science 277, 1306–1309.
[4] Momburg, F. and Tan, P. (2002) Mol. Immunol. 39, 217.
[5] Abele, R. and Tampé, R. (1999) Biochim. Biophys. Acta 1461, 405–419.
[6] Lankat-Buttgereit, B. and Tampé, R. (1999) FEBS Lett. 464, 108–112.
[7] Vos, J.C., Spee, P., Momburg, F. and Neefjes, J. (1999) J. Immunol. 163, 6679–6685.
[8] Meyer, T.H., van Endert, P.M., Uebel, S., Ehring, B. and Tampé, R. (1994) FEBS Lett. 351, 443–447.
[9] Urlinger, S., Kuchler, K., Meyer, T.H., Uebel, S. and Tampé, R. (1997) Eur. J. Biochem. 245, 266–272.
[10] Powis, S.J., Townsend, A.R., Deverson, E.V., Bastin, J., Butcher, G.W. and Howard, J.C. (1991) Nature 354, 528–531.
[11] Zhou, X., Glas, R., Momburg, F., Hämmerling, G.J., Jondal, M. and Ljunggren, H.G. (1993) Eur. J. Immunol. 23, 1796–1801.
[12] de la Salle, H., Zimmer, J., Fricker, D., Angenieux, C., Cazenave, J.P., Okubo, M., Maeda, H., Plebani, A., Tongio, M.M., Dormoy, A. and Hanau, D. (1999) J. Clin. Invest. 103, R9–R13.
[13] van Endert, P.M., Tampé, R., Meyer, T.H., Tisch, R., Bach, J.F. and McDevitt, H.O. (1994) Immunity 1, 491–500.
[14] Uebel, S., Meyer, T.H., Kraas, W., Kienle, S., Jung, G., Wiesmüller, K.H. and Tampé, R. (1995) J. Biol. Chem. 270, 18512–18516.
[15] Gorbulev, S., Abele, R. and Tampé, R. (2001) Proc. Natl. Acad. Sci. USA 98, 3732–3737.
[16] Alberts, P., Daumke, O., Deverson, E.V., Howard, J.C. and Knittler, M.R. (2001) Curr. Biol. 11, 242–251.
[17] van Endert, P., Saveanu, L., Hewitt, E. and Lehner, P. (2002) Trends Biochem. Sci. 27, 454.
[18] Neumann, L., Abele, R. and Tampé, R. (2002) J. Mol. Biol., in press.
[19] Frillingos, S., Sahin-Toth, M., Wu, J. and Kaback, H.R. (1998) FASEB J. 12, 1281–1299.
[20] Neefjes, J.J., Momburg, F. and Hämmerling, G.J. (1993) Science 261, 769–771.
[21] Ahn, K., Meyer, T.H., Uebel, S., Sempe, P., Djaballah, H., Yang, Y., Peterson, P.A., Früh, K. and Tampé, R. (1996) EMBO J. 15, 3247–3255.
[22] Tomazin, R., Hill, A.B., Jugovic, P., York, I., van Endert, P., Ploegh, H.L., Andrews, D.W. and Johnson, D.C. (1996) EMBO J. 15, 3256–3266.
[23] Nijenhuis, M. and Hämmerling, G.J. (1996) J. Immunol. 157, 5467–5477.